Effective Removal of Asphaltene Deposition in Metal-Capillary Tubes

Sara M. Hashmi and **Abbas Firoozabadi,** Yale University

Summary

We describe asphaltene deposition and removal processes in metal capillaries. We induce asphaltene precipitation by adding an asphaltene precipitant, heptane, to a petroleum fluid. The mixture is then injected through a laboratory-scale capillary and allowed to deposit. We assess the reversal of the deposition by means of the use of two separate chemical treatments: (1) a strong organic acid surfactant and (2) an aromatic solvent. The strong organic acid surfactant, dodecyl benzene sulfonic acid (DBSA), was shown to completely dissolve asphaltenes by means of acid-base chemistry reactions at heteroatomic sites on the asphaltene molecules. We investigate the use of DBSA as an efficient removal agent, injecting it in a mixture of petroleum fluid after the deposit was already formed. An aromatic solvent, toluene, is also investigated in such a fashion to assess its ability in removing deposited asphaltenes. We find that DBSA can effectively remove asphaltene deposits within one pore-volume (PV) of injection and at concentrations roughly ten times less than that required by an aromatic solvent such as toluene. To the best of our knowledge, our current study is the first laboratory-scale investigation with surfactant chemicals to reverse asphaltene deposition in capillaries.

Introduction

Asphaltene deposition on metal surfaces causes problems in industrial settings: Because petroleum fluids are produced from reservoirs, depressurization can cause asphaltene precipitation, ultimately resulting in deposition. Even though this deposition can occur in both wellbores and pipelines, we confine our current investigation to the flow characteristics of capillaries. A few case studies were performed to measure the thickness of the deposited layer in well tubing with diameters of 4.5 and 1.75 in. (Haskett and Tartera 1965; Al-Kafeef et al. 2005). In one case, asphaltene deposition in a west Kuwait well was assessed through measurements of flowing wellhead pressure by a pressure gauge, and found to reach one-third of the inner well-tubing radius (Al-Kafeef et al. 2005). In another case, with a similar method, the deposit in five different wells of the Hassi Messaoud field in Algeria was measured, and found to reach approximately two-thirds of the inner-tubing radius (Haskett and Tartera 1965). Such excessive deposition greatly reduces production efficiency. Costly shutdowns are often required to restore full operation. Furthermore, some wells can become plugged again within 1 to 3 months after chemical treatments are applied (Al-Sahhaf et al. 2002). Asphaltene precipitation can be prevented by the addition of large amounts of aromatic solvents or smaller amounts of strong organic acid surfactants. Depending on the type of surfactant and its dosage, surfactants can stabilize asphaltenes in bulk colloidal suspensions or dissolve them into molecular solutions (Hashmi and Firoozabadi 2011, 2012, 2013; Hashmi et al. 2012). Asphaltene deposits can be removed by large amounts of aromatic solvents, such as mixed xylenes or, in some cases, toluene. The purpose of this paper is to investigate the use of strong organic acids as low-dosage removal agents. Furthermore, we investigate the effectiveness of treatment in flow conditions. Although conventional treatments often involve soaking, this requires stoppage of the flow. Effective remediation treatments deployed during flow may greatly reduce stoppage time.

Asphaltenes are the most highly aromatic molecules in petroleum fluids. As such, they have a tendency to precipitate out of solution under a variety of conditions. In the field, this precipitation occurs mainly as a function of depressurization from reservoir conditions. Precipitation also can occur after the mixing of different petroleum fluids. In fact, asphaltenes have an operational definition that is based on compositional dependence: They are soluble in aromatics such as toluene, but insoluble in medium-chain alkanes such as heptane. The phenomenon of asphaltene precipitation is coupled with deposition on metallic surfaces in wellbores and pipelines. The chemical nature of asphaltenes and their interactions with dispersants play an important role in determining the effectiveness of dispersants in treating asphaltene deposition. The aromaticity of asphaltenes and their ability and propensity to associate on a molecular level lend clues to the chemistry required to prevent or otherwise inhibit their precipitation. Although large amounts of aromatic solvents can prevent precipitation, certain types of functionalized chemicals may be effective at much lower concentrations.

In addressing asphaltene precipitation, several different types of dispersants and surfactants were investigated in the literature, most notably strong organic acids such as DBSA and other long-chain organic surfactants such as nonyl-phenol (Chang and Fogler 1994a, b; Al-Sahhaf et al. 2002). Most studies investigate the effect of dispersants on the onset of asphaltene deposition, measured in terms of the amount of precipitant required to induce asphaltene precipitation (Permsukarome et al. 1997; Kaminski et al. 2000; Ostlund et al. 2004). Strong organic acids, in particular DBSA, are found to work by attacking heteroatomic sites in asphaltene molecules (Hashmi et al. 2012; Hashmi and Firoozabadi 2013). The resultant acid-base interactions along the long-chain carbon tails of DBSA form a solvation shell around the asphaltene molecules, thereby dissolving them (Leon et al. 1999; Rogel and Leon 2001).

Strong organic acids such as DBSA can fully dissolve precipitated asphaltenes to the molecular level, despite the presence of excess asphaltene precipitant such as heptane. This dissolution occurs through a chemical process, by protonation of heteroatomic content in the asphaltenes (Hashmi et al. 2012). Lone electron pairs on the asphaltenes bond with the protons that disassociate from the acid, and the resultant ion pairs formed by the disassociating acid remain closely complexed to each other through electrostatic interactions (Hashmi et al. 2012). When DBSA is present in small concentrations, less than 1,000 ppm, it can stabilize colloidal asphaltenes from several different petroleum fluids (Hashmi et al. 2012; Hashmi and Firoozabadi 2013). Colloidal stabilization by slightly larger amounts of DBSA is accompanied by partial asphaltene dissolution (Hashmi et al. 2012; Hashmi and Firoozabadi 2013). At higher concentrations, near 5% by weight, DBSA can fully dissolve precipitated asphaltene content in at least three different petroleum fluids (Hashmi et al. 2012; Hashmi and Firoozabadi 2013). Because of the chemistry that occurs between DBSA and asphaltenes, DBSA is not a true asphaltene solvent such as toluene: DBSA does not act purely through bulk thermodynamics.

On the laboratory scale, several experimental works investigated asphaltene deposition in metal-capillary tubing. In straight

This paper (SPE 166404) was accepted for presentation at the SPE Annual Technical Conference and Exhibition, New Orleans, 30 September–2 October 2013, and revised for publication. Original manuscript received for review 24 December 2013. Revised manuscript received for review 24 September 2015. Paper peer approved 4 January 2016.

Petroleum Fluid	f (g/g)	μ (Pa·s)	ρ (g/cm^3)	Onset (heptane)	Water Content
CVA	0.0803 [0.0504]	0.0308	0.8798	25% by volume	2,750 ppm

Capillary	L (cm)	R_0 (cm)	V (cm^3)
—	30	0.05	0.23

Table 1—Material properties for the CVA petroleum fluid and geometric characteristics of the capillary. The value of f in brackets indicates that obtained with the capillary flow composition conditions.

metal-capillary studies, pressure drop is monitored as an indication of the constriction of the conduit (Nabzar and Aguilera 2008; Hoepfner et al. 2013). In larger metal pipes (24-mm diameter), decreasing flow rate and increasing asphaltene content were both found to increase deposition (Soulgani et al. 2009). Evidence was presented to suggest both that deposition is uniform throughout a given length of pipe and that deposition occurs mainly near the pipe inlet (Wang et al. 2004; Nabzar and Aguilera 2008; Soulgani et al. 2009; Hoepfner et al. 2013). Changes in composition and temperature can reveal the thermodynamic envelope for depositing asphaltenes inside capillaries (Broseta et al. 2000; Wang et al. 2004). Despite these investigations of asphaltene deposition in capillaries, however, investigations of asphaltene-deposit removal by chemical means remain lacking.

In this study, we investigate an effective low-dosage chemical from the literature in a laminar capillary asphaltene deposition study. We choose DBSA, arguably the most effective of the strong organic acids thus far investigated in the asphaltene literature (Chang and Fogler 1994a; Permsukarome et al. 1997; Hashmi et al. 2012). We precipitate asphaltenes by co-injecting a petroleum fluid with heptane into a metal capillary, and assess the resulting deposition. The strong organic acid DBSA can help remove asphaltene deposits when injected into a capillary in which asphaltenes were already deposited. In comparison with an asphaltene solvent, toluene, DBSA is equally effective at 10-times lower doses. To the best of our knowledge, our current study is the first laboratory-scale investigation demonstrating that certain chemicals can be effective low-dosage inhibitors or dissolution agents to treat asphaltene deposition in metal capillaries.

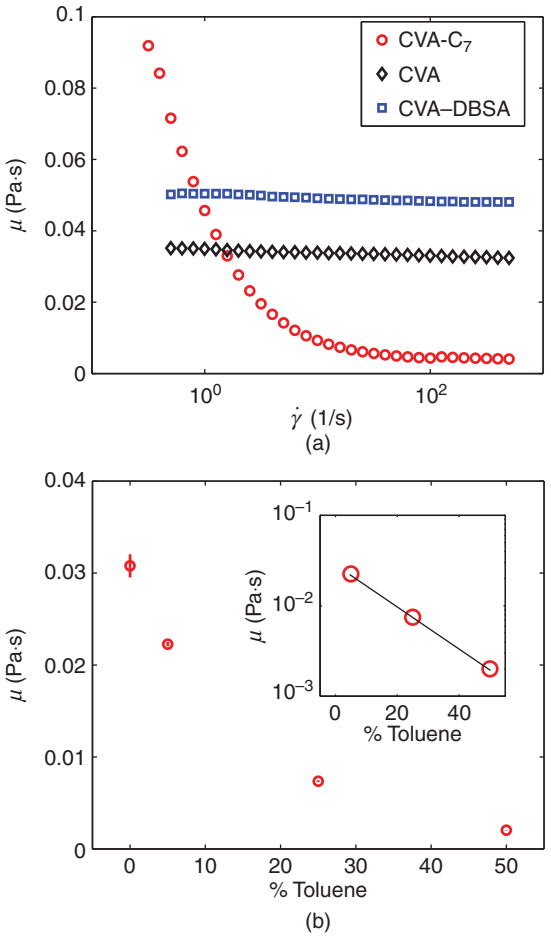

Fig. 1—Bulk rheological characteristics: (a) shows viscosity μ as a function of shear rate $\dot{\gamma}$ for CVA, CVA mixed in equal volumes with heptane, and 5% DBSA mixed with CVA. (b) Gives μ of CVA as a function of toluene content, including the measurement of pure CVA shown in (a). The inset in (b) shows μ on a log scale, indicating an Arrhenius-type behavior, where the black line denotes $\mu = \mu_0 \exp(-0.054x)$, where x is the toluene concentration and $\mu_0 = 0.0308$ is the viscosity of CVA alone.

Materials and Methods

Materials. We obtain and use a petroleum fluid called CVA to assess asphaltene deposition in a metal capillary. The onset of asphaltene precipitation in CVA occurs at approximately 25% volume of heptane, as indicated by a spot test within several minutes after mixing. Even though asphaltene deposits in the field may be caused by changes in pressure or temperature or by interactions with produced brine, we induce asphaltene precipitation on the laboratory scale by mixing CVA with heptane, and quantify the amount of asphaltenes precipitated from the mixture. We characterize CVA by its density $\rho = 0.8798$ g/cm^3, asphaltene mass fraction $f = 0.0803$, and viscosity $\mu = 0.0345$ Pa·s. We measure ρ (g/cm^3) with a densitometer (Anton Paar DMA 5000). We measure f by means of filtration, with a heptane ratio $\chi = 40$ cm^3/g: 1 g of petroleum fluid is mixed with 40 cm^3 of heptane [high-performance liquid chromatography (HPLC) grade, JT Baker], allowed to precipitate overnight, and then is filtered to recover the asphaltene fraction f. We also report $f = 0.0504$, obtained by filtering an equi-volume mixture of CVA and heptane, to mimic the conditions encountered in the metal capillaries. We measure the water content of CVA to be 2,750 ppm, by means of a Karl Fischer titration in Hydranal Coulomat solution (Sigma Aldrich). **Table 1** summarizes the properties of CVA. We obtain DBSA and HPLC-grade toluene from Acros Organics.

We measure the viscosity μ with a rheometer (Anton Paar MCR 301), in a cone-and-plate geometry (CP25), over a range of shear rates $\dot{\gamma}$. **Fig. 1a** shows the rheological behavior of CVA and mixtures of CVA with heptane at a 1:1 volume ratio and with DBSA at 5%. The petroleum fluid is Newtonian, shown by the open black diamonds, as is the mixture of CVA with 5% DBSA, shown by the open blue squares. DBSA has a viscosity of 1.3 Pa·s, and so the mixture of 5% DBSA in CVA results in an increase of μ by a factor of ≈1.5. The equi-volume mixture of CVA and heptane (open red circles) shear thins at less than ≈100 seconds^{-1}. At $\dot{\gamma} = 500$ seconds^{-1}, μ for CVA-heptane is also approximately an order of magnitude less than CVA itself. Asphaltene precipitation is known to result in unstable, quickly aggregating suspensions (Hashmi and Firoozabadi 2010). The shear thinning in CVA-heptane is caused by the shear-induced breakup of the unstable colloidal suspension, as is observed in colloidal gels (Poon et al. 1999; Starrs et al. 2002). Mixtures of CVA with toluene, similar to the mixture of CVA with DBSA, are Newtonian fluids that do not result in precipitation. Toluene has a viscosity of 5.9×10^{-4} Pa·s: The mixture of 5% toluene with CVA results in a decreased viscosity by a factor of ≈1.7, while the mixture of 50% toluene with CVA results in a decrease in μ by a factor of approximately 15. Fig. 1b shows the average Newtonian μ for mixtures of CVA with toluene as a function of the volume percentage of toluene, including the measurement of pure

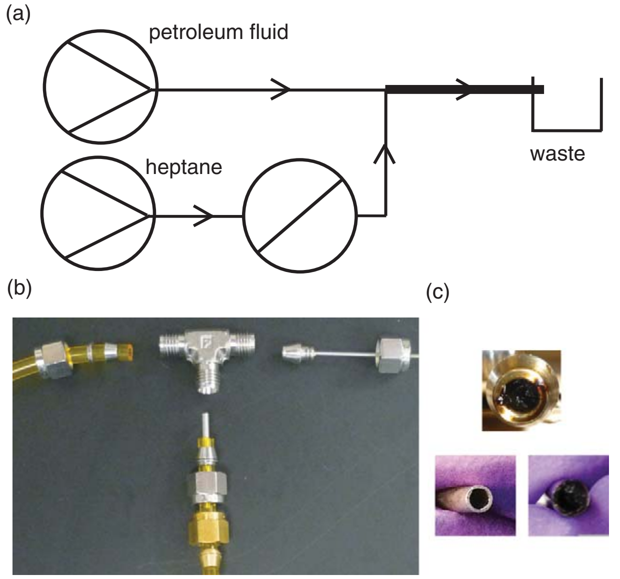

Fig. 2—Flow setup and schematic: (a) shows a diagram of the setup, with arrows indicating the direction of flow from the syringe-pump inputs to the output waste. The syringe pumps are each indicated by a circle surrounding an arrowhead, the transducer by a circle with a single line, and the capillary by the thick black line at the outlet of the T-junction. (b) Shows a picture of the nozzle used at the T-junction in (a), which allows for better mixing of the two fluids. (c) shows images of the capillary. At the top is an image of the inlet after deposition, and the bottom images show the outlet both before (left) and after (right) deposition.

CVA, as shown in Fig. 1a. The inset in Fig. 1b shows the same viscosity data on a log scale, indicating an Arrhenius-type behavior caused by the effective decrease in asphaltene content with the addition of toluene. The black line denotes $\mu = \mu_0 \exp(-0.054x)$, where x is the toluene concentration by volume and $\mu_0 = 0.0308$ Pa·s is the viscosity of CVA alone. All materials characterizations are performed at room temperature.

Methods. In this study, we use a stainless-steel capillary (McMaster-Carr) with length $L = 30$ cm, radius $R_0 = 0.05$ cm, and volume $V = 0.23$ cm^3, as tabulated in Table 1. Flow is driven through the capillary at a constant total-volume flow rate Q from two syringe pumps (KD Scientific). A pressure transducer (Omega) is placed at the inlet of the capillary to measure the total pressure drop ΔP. The outlet of the capillary is open to atmospheric pressure. A schematic of the setup is given in **Fig. 2a.** The arrows indicate the direction of flow. The syringe pumps are each indicated by a circle surrounding an arrowhead, the transducer by a circle with a single line, and the capillary by the thick black line at the outlet of the T-junction. Fig. 2b shows an exploded image of the junction, including a small metal nozzle that is inserted in the heptane line to enhance mixing in the T-junction. Fig. 2c shows images of the capillary inlet (top) after a typical deposition run, and the capillary outlet (bottom) both before (left) and after (right) a deposition run. After the experimental runs were completed for data collection, we performed a final deposition run and then cut the capillary open to inspect cross sections at the entrance, middle, and exit. As in other examples of asphaltene deposition in the literature, we observe deposition throughout the length of the capillary (Kraiwattanawong et al. 2009). All deposition and removal runs are performed at room temperature.

To deposit asphaltenes inside the capillary, we use one syringe pump to inject CVA, and the second to co-inject an equal volume of heptane. To study the removal effect of DBSA and toluene, we prepare both stock solutions of DBSA added directly to CVA, and stock solutions of toluene added directly to CVA. We begin the experiment with a deposition run, in which one syringe pump injects heptane and the other syringe pump injects an equal volume of CVA. All deposition runs are carried out at fixed $Q = 0.7$ cm^3/min, with shear rate ≈ 30 seconds^{-1} and Reynolds number $Re = 2\rho QR/A\mu \sim 5$, where R is the inner radius of the capillary, A its cross-sectional area, and μ the viscosity of the mixture.

At the end of the deposition run, the heptane injection stops, and the CVA injection is replaced by CVA or a stock solution of CVA with either DBSA or toluene. We call this the "removal run." We use CVA on its own as a removal agent as a control to assess the effect of shear ablation in the absence of chemical dissolution. To investigate the effectiveness of DBSA, we prepare stock solutions of 2.5 and 5% by volume in CVA. To investigate the effectiveness of toluene, we use stock solutions at 5, 25, and 50% by volume in CVA. The removal runs with 5% DBSA are carried out at flow rates $Q = 0.035$, 0.07, 0.175, and 0.35 cm^3/min, whereas the removal runs with 25% toluene are carried out at flow rates $Q = 0.035$, 0.07, and 0.14 cm^3/min. To compare the effect of the two concentrations of DBSA and the three concentrations of toluene, we fix $Q = 0.07$ cm^3/min, and duplicate the runs two to three times. In the removal runs, Re ranges from 0.5 to 10, and the largest shear forces are encountered with the highest viscosity fluid, namely, 5% DBSA dissolved in the CVA. At the end of each removal run, we dismantle the capillary, transducer, and nozzle, and rinse all parts with toluene to dissolve any remaining asphaltene deposit. We use the same capillary from one set of deposition-removal experiments to the next. The toluene cleaning in between runs recovers the initial pressure-drop behavior, suggesting no permanent effect of deposition on the inner surface of the capillary.

To validate the capillary flow setup, we run several control experiments. In the first control experiment, we flow a pure petroleum fluid through the capillary to ensure that asphaltene deposition does not occur. **Fig. 3a** shows the resulting constant pressure drop ΔP for CVA flowing at $Q = 0.7$ cm^3/min. In the second control, we validate that the flow is laminar, governed by the Poiseuille equation,

$$\Delta P = \frac{8\mu QL}{\pi R^4}, \quad (1)$$

where L is the length of the capillary. We flow heptane alone through the capillary at different flow rates and measure the pressure drop as a function of Q. The result is linear, as expected, with a slope 7.2×10^{-3} [psi/(cm^3/min)]. To further validate the assumption of laminar flow, we also investigate the CVA-heptane mixture at different flow rates, and measure ΔP_0, the initial pressure drop before the onset of deposition, as a function of Q. Fig. 3b shows the results for ΔP_0 (Q) for heptane and the CVA-heptane mixture. The solid lines are measured slopes of the data. Comparing the measured slopes to those predicted by Eq. 1, the deviations range from 30 to 70%. The discrepancy could arise from the T-junction, which is beyond the pressure transducer, but with a geometry that is not accounted for in Eq. 1. It could also arise from the tolerance on the capillary radius: A tolerance of 10% on the capillary radius itself could lead to a 45% difference in the slope of ΔP_0 as a function of Q.

Results and Discussion

Deposition. In the absence of an inhibitory chemical, the precipitating CVA/heptane mixture generates asphaltene deposition on the capillary walls. Because the deposit occludes the capillary, the pressure drop increases. We assess deposition by measuring ΔP across the capillary as a function of injected PVs. **Fig. 4** shows five typical examples of ΔP(PV) for CVA-heptane mixtures at $Q = 0.7$ cm^3/min. Each mixture exhibits some stochastic behavior indicating that some portions of the deposit may experience removal or rearrangement. During 12 runs, each consisting of approximately 460 PV, the initial pressure drop varies by a few percent: $\Delta P_0 = 0.16 \pm 0.01$ psi, a 6% variation. The excess pressure drop attained at PV $\approx$ 460 is $\Delta P - \Delta P_0 = 0.88 \pm 0.28$, a

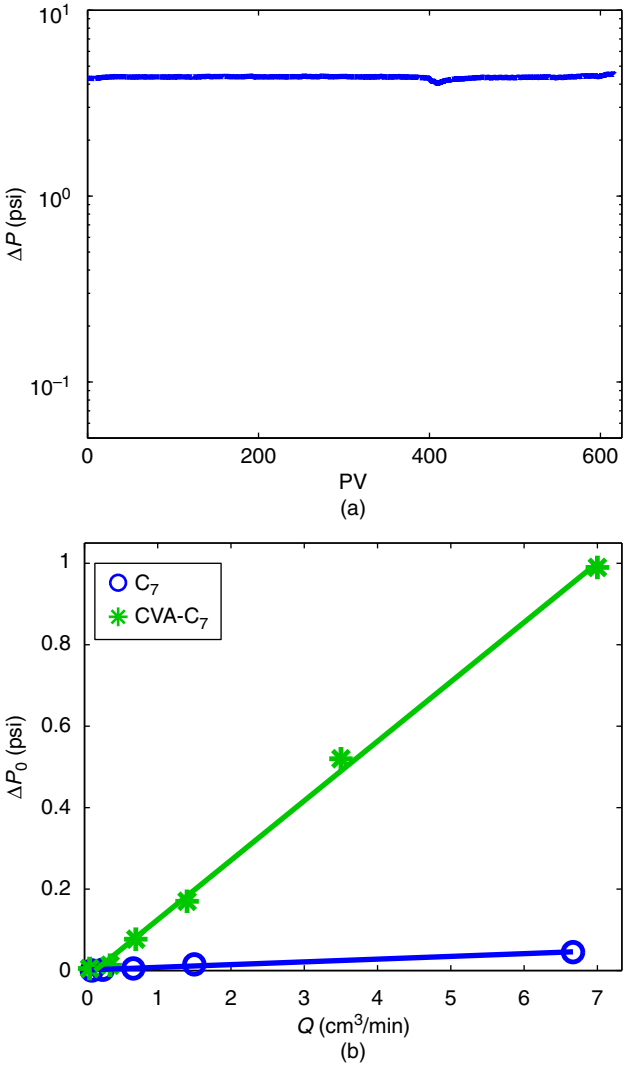

Fig. 3—Control runs: (a) shows a trace of ΔP for CVA flowing through the capillary without mixing with or precipitation by heptane, at $Q = 0.7$ cm^3/min; (b) shows ΔP_0 for heptane (blue circles) and for the equi-volume CVA/heptane mixture before the onset of precipitation (green stars) as a function of Q.

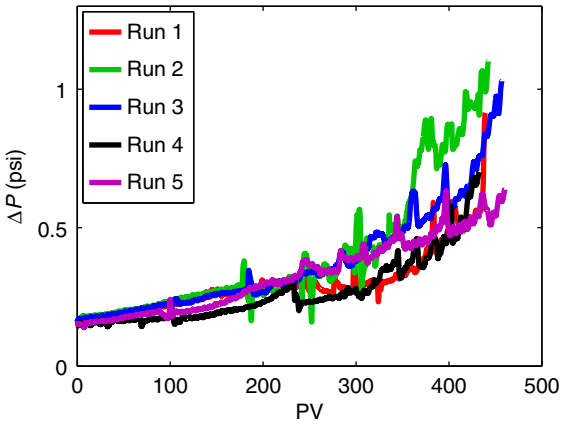

Fig. 4—Five typical traces of ΔP during the deposition phase, plotted as a function of PV injected. Each run consists of an equi-volume mixture of CVA and heptane, at a flow rate $Q = 0.7$ cm^3/min.

variation of ≈32%. Fig. 4 shows five typical runs. With the average ΔP attained in the deposition runs and with the assumption that the deposition is uniform in the axial and radial directions, we can use Eq. 1 to estimate the amount of clogging that results. We find $R_d/R_0 = (\Delta P/\Delta P_0)^{-1/4} \approx 64 \pm 4\%$ at the end of the deposition runs, meaning that the deposition extends to roughly one-third of the capillary radius. The similarity between successive deposition runs after complete cleaning of the capillary suggests the absence of any corrosion on the inner surface of the capillary.

Removal. To assess removal, we begin with a deposition run, followed by an injection of a nondepositing fluid—namely, the petroleum fluid CVA with chemical additives—but without the addition of heptane. We use nondepositing fluids as removal agents to isolate the effects of deposition and removal. **Fig. 5a** shows an example of a depositing injection followed by a removal injection. In this case, we plot ΔP as a function of time t, and shift the time axis so that $t = 0$ indicates the beginning of the removal portion of the run. At the beginning of the run, the capillary is clean, with the initial radius R_0, as indicated in the cartoon in Fig. 5b. The deposition run is carried out at $Q = 0.7$ cm^3/min for approximately 500 PV. During deposition, ΔP rises to 0.65 psi. The rise in ΔP indicates the occlusion of the capillary from the original R_0 to R_d, the radius after deposition, as shown in the cartoon in Fig. 5b. The removal run is shown with a dashed blue line, and for the example in Fig. 5a, the removal conditions are given by $Q = 0.07$ cm^3/min; the injected fluid is CVA with 5% DBSA. ΔP decreases as the deposit is removed, indicating the removal of the asphaltene deposit and the opening of the radius from R_d to R, as indicated in the cartoon in Fig. 5b.

At the onset of the removal run shown in Fig. 5a, the initial $\Delta P_i = 0.23$ psi rather than $\Delta P = 0.65$ psi from the end of the deposition run, because of the mismatch in flow conditions, both Q and μ, between the two runs. The deposition run occurs at $Q = 0.7$ cm^3/min, and the fluid mixture has a viscosity of 0.010 Pa·s. In the removal run, $Q = 0.07$ cm^3/min, and the fluid mixture has a viscosity of 0.048 Pa·s. When the geometry of the capillary stays constant between the end of the deposition run and the beginning of the removal run, Eq. 1 therefore predicts the pressure-drop mismatch between the two runs to be a factor of $(\Delta P)_{rem}/(\Delta P)_{dep} = (Q\mu)_{rem}/(Q\mu)_{dep} = 0.48$. In fact, the observed mismatch is a factor of 0.36, within 25% of the predicted value. The discrepancy between the observed and predicted values of the pressure-drop mismatch may indicate a slight rearrangement of the deposit occurring between the deposition and removal runs. For the CVA with 5% DBSA, four different flow rates were used, whereas for CVA with 25% toluene, three different flow rates were used. To compare results from the five different compositions with each other, the removal flow rate is fixed at 0.07 cm^3/min.

In investigating the effectiveness of removal agents, DBSA and toluene, we first assess the effectiveness of a noninhibitory chemical, namely, the petroleum fluid CVA on its own. With the absence of chemical treatment in the pure petroleum fluid, these control runs assess the effect of deposit removal caused by physical means, namely, ablation by shear forces. We run the CVA control removal at $Q = 0.07$ cm^3/min to equal the flow rate used with all the chemical treatments. Furthermore, to differentiate the effects of shear removal from chemical removal, we also assess the effect of larger shear rates encountered in removal runs with the 5% DBSA mixture. Because of the higher viscosity of the 5% DBSA mixture, to obtain similar shear forces with CVA alone, we also use $Q = 0.56$ cm^3/min. **Fig. 6** shows five control runs in which CVA is used as the removal agent, by use of the two different flow rates as indicated in the legend, in cm^3/min. The traces of ΔP were normalized by ΔP_i, the initial pressure drop at the beginning of the removal run. Using this normalization corrects for the effects of the pressure-drop mismatching and allows for direct comparisons between runs of different compositions. Decreases in $\Delta P/\Delta P_i$ over PVs injected indicate removal of the deposit and subsequent reopening of the capillary. However, when the control fluid is used, $\Delta P/\Delta P_i$ decreases only to an average value of 0.90 ± 0.09, and there is no strong dependence on flow rate. This decrease represents an average change in the capillary radius from

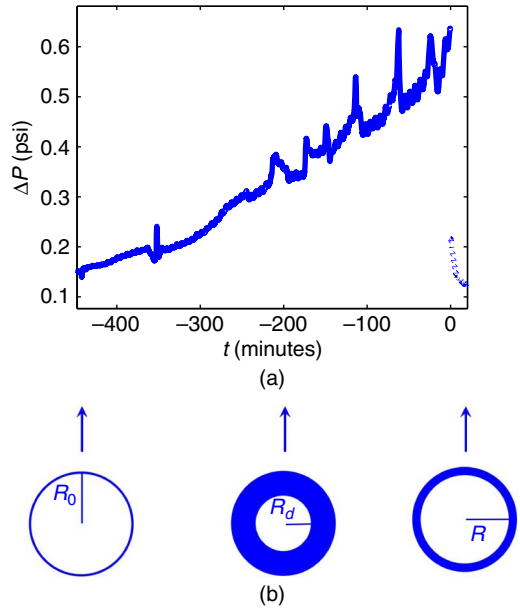

Fig. 5—(a) Shows an example of a full run including both the deposition and removal portions, as a function of time, where $t = 0$ is the time of switching between deposition and removal. The deposition run is shown in the solid blue line, whereas the removal run is shown by the hatched blue line starting at $t = 0$ and $\Delta P \approx 0.23$ psi. (b) Shows a depiction of the cross section of the capillary as deposition occurs and then reverses after treatment for removal.

$R/R_0 = 0.64$ at the end of the deposition run to $R/R_0 = 0.66 \pm 0.02$ only. In particular, we note that the fastest flow-rate runs, exerting the largest shear forces onto the deposit, accomplish little, if any, removal of the deposited asphaltenes. Because shear ablation does not suffice for removal, chemical means are required to effectively remove the deposit, which we investigate next.

To test the consistency of removal by chemical means, we use a mixture of 5% DBSA with the petroleum fluid CVA to remove asphaltene deposits from inside the capillary. **Fig. 7** shows three traces of 5% DBSA removing asphaltene deposits during one PV injection after deposition. Runs 2 and 3 show mainly smooth behavior, whereas Run 1 exhibits a degree of stochasticity in the removal behavior, reminiscent of that observed in the deposition behavior. In all three of the traces, $\Delta P/\Delta P_i$ has decreased to approximately 50% after just one-fourth of a PV injection. After one PV was injected, $\Delta P/\Delta P_i$ decreased to $34 \pm 4\%$, for a run-to-run variation of $\approx 12\%$. The decrease in $\Delta P/\Delta P_i$ after one PV corresponds to a cleaning of the capillary from the average occluded

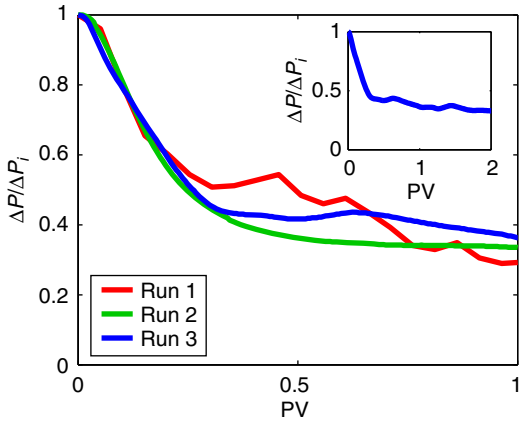

Fig. 7—Run-to-run variation: Three traces of $\Delta P/\Delta P_i$ during the rinsing phase, by use of 5% DBSA in CVA at $Q = 0.07$ cm^3/min. The inset shows the trace of Run 3 for the first 2 PV injected.

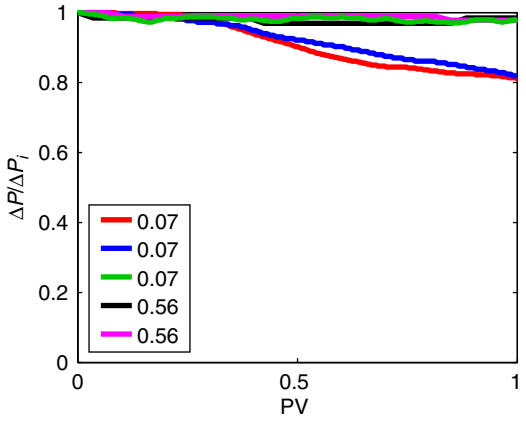

Fig. 6—Rinsing control run: Each trace of $\Delta P/\Delta P_i$ indicates a run during the rinsing phase, by use of CVA alone and Q as indicated in the legend, in cm^3/min.

radius $R_d/R_0 \approx 64 \pm 4\%$ to $R/R_0 \approx 84 \pm 3\%$, removing nearly 60% of the deposited asphaltene thickness with just a 1-PV injection. In general, most of the removal is observed during the first-PV injection. Run 3 exemplifies this, as shown in the inset to Fig. 7, which shows the first 2 PV injected.

Likewise, **Fig. 8** shows three traces of 25% toluene in CVA. After one PV injected, $\Delta P/\Delta P_i$ decreases to $50 \pm 14\%$, for a run-to-run variation of less than 30%. The decrease in $\Delta P/\Delta P_i$ after 1 PV corresponds to a cleaning of the capillary from the average occluded radius $R_d/R_0 \approx 64 \pm 4\%$ to $R/R_0 \approx 77 \pm 5\%$, removing approximately 36% of the deposited asphaltene thickness with a 1-PV injection. As also seen with DBSA, most of the removal is accomplished during the first PV injected, again, as shown with the first 2 PV injected for Run 3, in the inset to Fig. 8.

We inject 5% DBSA-CVA mixtures to remove deposited asphaltenes, and investigate the effect of flow rate as a function of PVs injected. **Fig. 9** shows the traces of $\Delta P/\Delta P_i$ for flow rates $0.035 < Q < 0.3$ cm^3/min, where each trace represents a single run. Here, the normalization by ΔP_i corrects for differences in the pressure-drop mismatch caused by differences in the flow rate. Each of the four flow rates succeeds in reducing $\Delta P/\Delta P_i$ to 0.26 ± 0.09 after 1 PV injected. Although the overall behavior is not highly dependent on Q, one can see a distinction between the runs at early times as the flow rate slows. After only 0.2 PV injected, the run with the slowest flow rate, $Q = 0.035$ cm^3/min, has accomplished the greatest degree of reduction in $\Delta P/\Delta P_i$. The comparison in Fig. 9 may suggest that the slowest flow rate and longest residence time allow the greatest degree of molecular

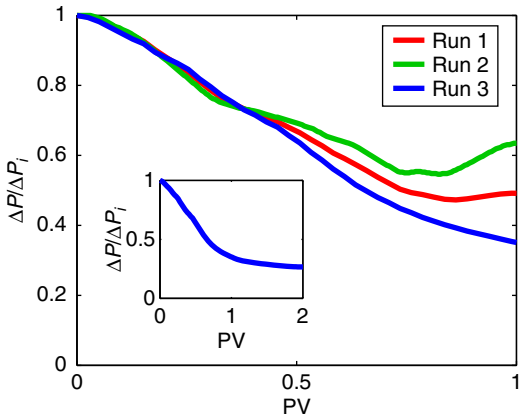

Fig. 8—Run-to-run variation: Three traces of $\Delta P/\Delta P_i$ during the rinsing phase, by use of 25% toluene in CVA at $Q = 0.07$ cm^3/min. The inset shows the trace of Run 3 for the first 2 PV injected.

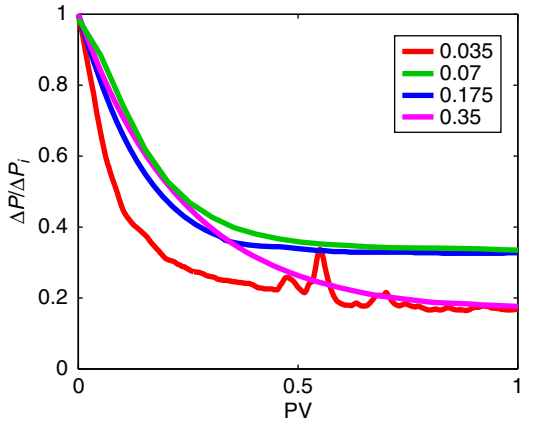

Fig. 9—The effect of flow rate by use of 5% DBSA mixed with CVA: $\Delta P/\Delta P_i$ as function of PVs injected for one run at each of the flow rates listed in the legend.

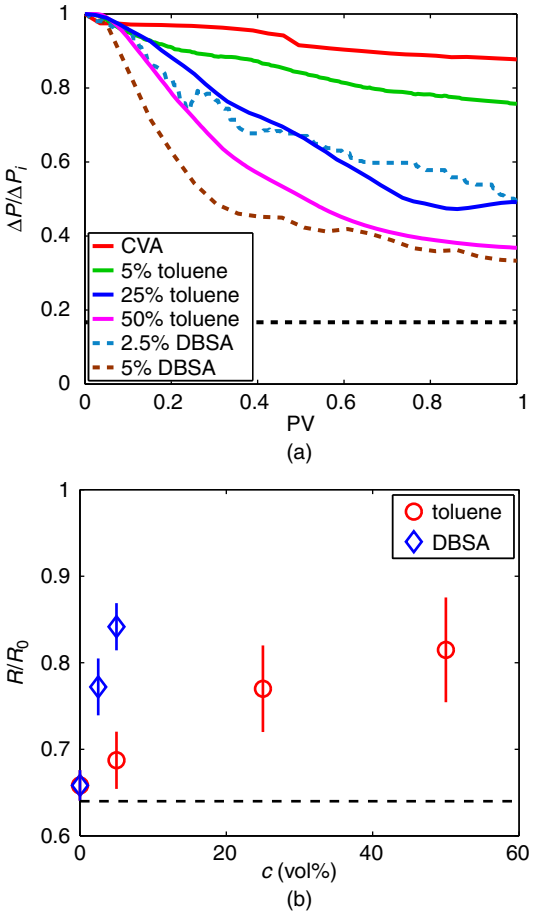

Fig. 10—Comparison of rinsing runs with toluene and DBSA. The six traces shown in (a) indicate the behavior of the CVA control run; the 5, 25, and 50% toluene mixtures in CVA; and the 2.5 and 5% mixtures of DBSA in CVA, as indicated in the legend. Each trace represents an average of 2 to 4 runs for each composition; all runs are at constant $Q = 0.07$ cm^3/min; the first PV injected is shown for all 6 traces of $\Delta P/\Delta P_0$. The horizontal black dashed line indicates the limit of a fully cleaned capillary. In (b), the extent of cleaning is represented by R/R_0 as a function of the concentration c of toluene and DBSA, as shown in the legend. The horizontal black dashed line indicates the average amount of deposition before the removal runs, whereas $R/R_0 = 1$ indicates a fully cleaned capillary.

contact between the DBSA and the deposited asphaltenes. The resultant removal may be caused by a combination of diffusive and chemical processes. Because convection is in the axial direction, diffusion rates control transport toward the wall (Hashmi et al. 2015). After contact with the deposit, DBSA acts by protonating the heteroatomic content of the asphaltenes to dissolve the deposit. This leads to a complexation of DBSA with asphaltene molecules, in which the long-chain alkane tails of the DBSA help to solvate asphaltenes (Hashmi et al. 2012; Hashmi and Firoozabadi 2013). The mechanism of acid-base chemistry is effective in dissolving precipitated asphaltenes in bulk solutions in the absence of flow (Al-Sahhaf et al. 2002). At higher Q, the flow may convect the DBSA away from the deposit before it has time to diffuse toward the asphaltene layer and chemically interact to dissolve the deposit.

By fixing the flow rate of the removal injection at $Q = 0.07$ cm^3/min, we can compare the effect of DBSA with various concentrations of toluene, and with the control run of CVA alone. **Fig. 10a** shows the results $\Delta P/\Delta P_i$ as a function of PV. Each trace now represents an average of two to four runs at the given composition. The normalization by ΔP_i corrects for differences in the pressure-drop mismatch because of the viscosity differences in the different compositions of chemical treatment. The comparison with the control indicates the importance of chemistry. Although the 5% DBSA treatment run has a higher viscosity than CVA alone, by a factor of 1.6, the shear forces exerted are still five-times less than the shear forces exerted by the control run operating at 0.56 cm^3/min and shown in Fig. 6. The results in Fig. 10 therefore indicate a comparison of the chemical effectiveness of DBSA and toluene. CVA on its own reduces $\Delta P/\Delta P_i$ by an average of only $11 \pm 9\%$ after PV = 1. Adding toluene to CVA improves the removal, as indicated by a greater decrease in $\Delta P/\Delta P_i$. At 5%, toluene reduces $\Delta P/\Delta P_i$ by $24 \pm 14\%$ within PV = 1, whereas 25% toluene reduces $\Delta P/\Delta P_i$ by $50 \pm 14\%$. Adding 50% toluene to CVA drastically improves the removal, reducing $\Delta P/\Delta P_i$ by $61 \pm 12\%$, with most of the pressure-drop reduction occurring within PV $\approx$ 0.5. Adding 2.5% DBSA to DBSA accomplishes comparable results to 25% toluene, with $\Delta P/\Delta P_i$ decreasing by $52 \pm 11\%$ after one PV injection. With 5% DBSA, a reduction in $\Delta P/\Delta P_i$ of more than 50% occurs within PV $\approx$ 0.4, and $\Delta P/\Delta P_i$ decreases by $66 \pm 4\%$ after 1 PV. Because the deposition runs result in clogging of the capillary to the extent $R_d/R_0 \approx 64 \pm 4\%$, a complete cleaning to restore the capillary back to its original, clean state should exhibit a pressure drop that falls to $\Delta P/\Delta P_i = (R_d/R_0)^4 = 0.17$. This limit is shown as the dashed black line in Fig. 10a.

In terms of the physical and chemical mechanisms of deposition and removal, the pressure-drop behavior can lend insight. For instance, the results in Fig. 10a suggest that the deposited layer inside the capillary may be thicker in the first 50% of the capillary length from the inlet. After PV reaches 0.4 to 0.6, the traces of $\Delta P/\Delta P_i$ begin to plateau for both the 5% DBSA and 50% toluene mixtures. A comparison between toluene and DBSA demonstrates the importance of chemistry. Interestingly, ten-times less DBSA added to CVA can accomplish the same result as toluene. This result suggests that a strong organic acid can be just as effective as a bulk solvent, but requiring smaller doses. Although the effect of DBSA is to solubilize asphaltene molecules in alkane environments by forming complexes containing long carbon tails, toluene must be present in a large enough excess to effectively modify the background solution. The acidity of DBSA also works to dissolve precipitated asphaltenes in bulk suspensions with a similar degree of effectiveness: 5% DBSA added to a precipitated bulk asphaltene suspension was shown to redissolve the asphaltene precipitate just as effectively as approximately 50% toluene (Hashmi et al. 2012).

Just as one can use pressure-drop traces in the deposition runs to estimate the extent of radial clogging through Eq. 1, we also can estimate the extent of deposition reversal from the pressure-drop traces upon chemical treatment and asphaltene removal. We estimate the cleaned radius R after one PV of treatment, as shown in the cartoon in Fig. 5b, with $R/R_d = (\Delta P/\Delta P_i)^{1/4}$. **Table 2** compiles the results for $\Delta P/\Delta P_i$ after 1 PV, along with the reduction

Removal Composition	Minimum $\Delta P/\Delta P_i$ at $PV<1$	Reduction in R/R_d	R/R_0
CVA	0.90 ± 0.09	0.03 ± 0.02	0.66 ± 0.02
CVA-toluene 5%	0.76 ± 0.13	0.07 ± 0.05	0.69 ± 0.03
CVA-toluene 25%	0.50 ± 0.14	0.20 ± 0.08	0.77 ± 0.05
CVA-toluene 50%	0.39 ± 0.12	0.27 ± 0.09	0.81 ± 0.06
CVA-DBSA 2.5%	0.48 ± 0.11	0.21 ± 0.05	0.77 ± 0.03
CVA-DBSA 5%	0.34 ± 0.04	0.32 ± 0.04	0.84 ± 0.03

Table 2—Summary of the efficacy of the different chemical treatments within the first PV injected, all at $Q = 0.07\,cm^3/min$ for the removal runs. The values represent averages on the basis of two to four runs for each composition.

in R/R_d and the comparable increase in R/R_0 for each of the chemical treatments tested in the removal process. The values in Table 2 are based on two to four runs for each composition tested. The control run of CVA alone results in $\Delta P/\Delta P_i = 0.89 \pm 0.09$ after 1 PV injected, whereas runs of 5% DBSA or 50% toluene mixed with CVA result in $\Delta P/\Delta P_i < 0.4$. With the decrease in $\Delta P/\Delta P_i$, the reversal of the occlusion with the control treatment with CVA alone is only 3%, still leaving the capillary with $R/R_0 \approx 66 \pm 2\%$. The reversal of the occlusion process improves with an increasing concentration of either DBSA or toluene dissolved in the CVA and used in a removal run. The most effective treatment, 5% DBSA, reverses the occlusion by more than 30%, cleaning the capillary to $R/R_0 \approx 84 \pm 3\%$ of its initial radius. Furthermore, 5% DBSA dissolved in CVA results in a reversal comparable to that achieved with 50% toluene, which cleans the capillary to $81 \pm 6\%$ of its initial radius after 1 PV injected. Fig. 10b shows the results for R/R_0 in graphical format, as a function of the volume percent c of additive chemicals toluene and DBSA dissolved in CVA, as indicated in the legend. The upper limit $R/R_0 = 1$ indicates a fully cleaned capillary, whereas the dashed horizontal black line indicates the deposited thickness R_d/R_0 before the removal treatments. Both DBSA and toluene succeed in increasing R back toward the clean-capillary limit of R_0, with DBSA accomplishing the task at 10-times lower in concentration than toluene.

In comparing the mechanism of action of the two chemicals, several points need to be considered. In general, acid-base chemistry occurs very quickly, caused by the high mobility of the proton from the disassociated acid (Rini et al. 2004; Belson and Cox 2005). In the case of DBSA, the long-chain tail solvates asphaltene molecules after a sufficient number of acid molecules is bound to the asphaltene (Hashmi et al. 2012). Toluene, on the other hand, interacts with asphaltenes through the π electrons (Spiecker et al. 2003). In this case, neither a chemical reaction nor solvation but rather an excess of aromatic toluene molecules in the surrounding fluid prevents precipitation through bulk thermodynamics. The results in Fig. 10a suggest that the speeds of 5% DBSA and 50% toluene in reducing the deposit are comparable to each other. In both cases, the speed of interaction with the asphaltenes is limited by the speed of diffusive transport to the interface of the deposit and the fluid layer. Toluene molecules (molecular weight $\approx$ 92) are smaller than DBSA molecules (molecular weight $\approx$ 327), and would be expected to diffuse more easily to the asphaltene surface. The comparable speed of removal by DBSA, despite its larger molecular size, suggests that the acid-base chemistry indeed enhances dissolution. A similar comparison is seen when dissolving asphaltenes in bulk suspensions: 5% of DBSA can dissolve precipitated asphaltenes while closer to 50% toluene is required to dissolve an equal amount of asphaltenes (Hashmi et al. 2012). The fact that the presence of flow in the current study does not alter the chemical effectiveness comparison indicates that DBSA may be more effective than toluene in both soaking and batch injection flow treatments.

Because of the acidic nature of DBSA, we must consider the possible adverse effects of corrosion. Care must be taken in field conditions in which water may be present, because DBSA is known to partition into the water phase (Tigges et al. 2010). DBSA may lower the pH of water and possibly induce corrosion. DBSA also may necessitate the addition of demulsifiers in downstream oil/water separation processes. Corrosion is also more likely to occur with large volumes of acidic or caustic chemicals, and also when chemicals are allowed to soak or remain in contact with pipes in the absence of flow. In the present study, not only do we use small doses of DBSA, but we also use DBSA treatments under flow conditions. Both of these considerations may explain why we do not observe corrosion in our experiments. It is worth noting that CVA contains approximately 0.3% water. Despite the presence of this small amount of water, DBSA does not cause corrosion of our capillary. The effect of large amounts of water and brine on the performance of DBSA is currently under investigation.

Conclusion

We conclude that strong organic acids such as DBSA can remove immature asphaltene deposits. Although both DBSA and toluene mixed with the petroleum fluid remove almost all the deposited material within approximately 1-PV injection, the concentration of DBSA required for deposit removal is approximately 10 times less than that required for aromatic solvents. The most effective removal is obtained under low flow conditions, allowing the chemicals to soak. By contrast, attempts at shear removal of the deposit are unsuccessful, even with a tenfold flow-rate increase. In addition, although the tests were performed in the same capillary, no obvious corrosion was observed. Even though the cost of organic acids may be greater than that of aromatic solvents, the lower concentrations required may provide economic benefit. Furthermore, lower doses require less energy for downstream separation, and the environmental impacts will be less.

Acknowledgments

The authors gratefully acknowledge funding from the member companies of the Reservoir Engineering Research Institute, and the assistance of John E. Wolff and Batsirai Swiswa in building the laboratory-scale apparatus and collecting data, respectively.

References

Al-Kafeef, S. F., Al-Mechanhi, F., and Al-Shammari, A. D. 2005. A Simplified Method to Predict and Prevent Asphaltene Deposition in Oil-well Tubings: Field Case. *SPE Prod & Fac* **20** (2): 126–132. SPE-84609-PA. http://dx.doi.org/10.2118/84609-PA.

Al-Sahhaf, T. A., Fahim, M. A., and Elkilani, A. S. 2002. Retardation of Asphaltene Precipitation by Addition of Toluene, Resins, Deasphalted Oil and Surfactants. *Fluid Phase Equilibria* **194–197:** 1045–1057. http://dx.doi.org/10.1016/S0378-3812(01)00702-6.

Belson, D. L. and Cox, M. 2005. *Lehninger Principles of Biochemistry*. New York, New York: W. H. Freeman and Company.

Broseta, D., Robin, M., Savvidis, T. et al. 2000. Detection of Asphaltene Deposition by Capillary Flow Measurements. Presented at the SPE/DOE Improved Oil Recovery Symposium, Tulsa, 3–5 April. SPE-59294-MS. http://dx.doi.org/10.2118/59294-MS.

Chang, C.-L. and Fogler, H. S. 1994a. Stabilization of Asphaltenes in Alphatic Solvents Using Alkylbenzene-Derived Amphiphiles. 1. *Langmuir* **10** (6): 1749–1757. http://dx.doi.org/10.1021/la00018a022.

Chang, C.-L. and Fogler, H. S. 1994b. Stabilization of Asphaltenes in Alphatic Solvents Using Alkylbenzene-Derived Amphiphiles. 2. *Langmuir* **10** (6): 1758–1766. http://dx.doi.org/10.1021/la00018a023.

Hashmi, S. M. and Firoozabadi, A. 2010. Effect of Dispersant on Asphaltene Suspension Dynamics: Aggregation and Sedimentation. *J. Physical Chemistry B* **114** (48): 15780–15788. http://dx.doi.org/10.1021/jp107548j.

Hashmi, S. M. and Firoozabadi, A. 2011. Tuing Size and Electrostatics in Nonpolar Colloidal Asphaltene Suspensions by Polymeric Adsorption. *Soft Matter* **7:** 8384–8391. http://dx.doi.org/10.1039/C1SM05384A.

Hashmi, S. M., Zhong, K., and Firoozabadi, A. 2012. Acid-Base Chemistry Enables Reversible Colloid-to-Solution Transition of Asphaltenes in Non-Polar Systems. *Soft Matter* **8:** 8778–8785. http://dx.doi.org/10.1039/C2SM26003D.

Hashmi, S. M. and Firoozabadi, A. 2012. Field- and Concentration-Dependence of Electrostatics in Non-Polar Colloidal Asphaltene Suspensions. *Soft Matter* **8:** 1878–1883. http://dx.doi.org/10.1039/C2SM06865F.

Hashmi, S. M. and Firoozabadi, A. 2013. Self-Assembly of Resins and Asphaltenes Facilitates Asphaltene Dissolution by an Organic Acid. *J. Colloid and Interface Science* **394:** 115–123. http://dx.doi.org/10.1016/j.jcis.2012.11.069.

Hashmi, S. M., Loewenberg, M., and Firoozabadi, A. 2015. Colloidal Asphaltene Deposition in Laminar Pipe Flow: Flow Rate and Parametric Effects. *Physics of Fluids* **27:** 083302. http://dx.doi.org/10.1063/1.4927221.

Haskett, C. E. and Tartera, M. 1965. A Practical Solution to the Problem of Asphaltene Deposits —Hassi Messoud Field, Algeria. *J Pet Technol* **17** (4): 387–391. SPE-994-PA. http://dx.doi.org/10.2118/994-PA.

Hoepfner, M. P., Limsakoune, V., Chuenmeechao, V. et al. 2013. A Fundamental Study of Asphaltene Deposition. *Energy & Fuels* **27** (2): 725–735. http://dx.doi.org/10.1021/ef3017392.

Kaminski, T. J., Fogler, H. S., Wolf, N. et al. 2000. Classification of Asphaltenes via Fractionation and the Effect of Heteroatom Content on Dissolution Kinetics. *Energy and Fuels* **14** (1): 25–30. http://dx.doi.org/10.1021/ef990111n.

Kraiwattanawong, K., Fogler, H. S., Gharfeh, S. G. et al. 2009. Effect of Asphaltene Dispersants on Aggregate Size Distribution and Growth. *Energy & Fuels* **23** (3): 1575–1582. http://dx.doi.org/10.1021/ef800706c.

Leon, O., Rogel, E., Urbina, A. et al. 1999. Study of the Adsorption of Alkyl Benzene-Derived Amphiphiles on Asphaltene Particles. *Langmuir* **15** (22): 7653–7657. http://dx.doi.org/10.1021/la9812370.

Nabzar, L. and Aguilera, M. E. 2008. The Colloidal Approach. A Promising Route for Asphaltene Deposition Modelling. *Oil and Gas Science and Technology* **63** (1): 21–35. http://dx.doi.org/10.2516/ogst:2007083.

Ostlund, J.-A., Nyden, M., Fogler, H. S. et al. 2004. Functional Groups in Fractionated Asphaltenes and the Adsorption of Amphiphilic Molecules. *Colloids and Surfaces A: Physiochemical & Engineering Aspects* **234** (1–3): 95–102. http://dx.doi.org/10.1016/j.colsurfa.2003.12.013.

Permsukarome, P., Chang, C., and Fogler, H. S. 1997. Kinetic Study of Asphaltene Dissolution in Amphiphile/Alkane Solutions. *Industrial & Engineering Chemical Research* **36** (9): 3960–3967. http://dx.doi.org/10.1021/ie970177a.

Poon, W. C. K., Starrs, L., Meeker, S. P. et al. 1999. Delayed Sedimentation of Transient Gels in Colloid-Polymer Mixtures: Dark-Field Observation, Rheology and Dynamic Light-Scattering Studies. *Faraday Discussions* **112:** 143–154. http://dx.doi.org/10.1039/A900664H.

Rini, M., Pines, D., Magnes, B.-Z. et al. 2004. Bimodal Proton Transfer in Acid-Base Reactions in Water. *J. Chemical Physics* **121:** 9593–9610. http://dx.doi.org/10.1063/1.1804172.

Rogel, E. and Leon, O. 2001. Study of the Adsorption of Alkyl-Benzene-Derived Amphiphiles on an Asphaltene Surface Using Molecular Dynamics Simulations. *Energy and Fuels* **15** (5): 1077–1086. http://dx.doi.org/10.1021/ef000152f.

Soulgani, B. S., Rashtchian, D., Tohidi, B. et al. 2009. Integrated Modelling Methods for Asphaltene Deposition in Wellstring. *J. Japanese Petroleum Institute* **52** (6): 322–331. http://dx.doi.org/10.1627/jpi.52.322.

Spiecker, P. M., Gawrys, K. L., and Kilpatrick, P. K. 2003. Aggregation and Solubility Behavior of Asphaltenes and Their Subfractions. *J. Colloid and Interface Science* **267** (1): 178–193. http://dx.doi.org/10.1016/S0021-9797(03)00641-6.

Starrs, L., Poon, W. C. K., Hibberd, D. J. et al. 2002. Collapse of Transient Gels in Colloid-Polymer Mixtures. *J. Physics: Condensed Matter* **14** (10): 2485–2505. http://dx.doi.org/10.1088/0953-8984/14/10/302.

Tigges, B., Dederichs, T., Moller, M. et al. 2010. Interfacial Properties of Emulsions Stabilized With Surfactant and Nonsurfactant Coated Boehmite Nanoparticles. *Langmuir* **26** (23): 17913–17918. http://dx.doi.org/10.1021/la102761k.

Wang, J., Buckley, J. S., and Creek, J. L. 2004. Asphaltene Deposition on Metallic Surfaces. *J. Dispersion Science and Technology* **25** (3): 287–298. http://dx.doi.org/10.1081/DIS-120037697.

Sara M. Hashmi is an associate research scientist in the Yale University School of Engineering and Applied Science. Her research interests include fluid dynamics and a broad range of soft-materials investigations. Hashmi holds an AB degree in physics from Harvard University, and MS and PhD degrees in chemical and environmental engineering from Yale University.

Abbas Firoozabadi is senior scientist at RERI and a faculty member at Yale University. His research focus includes: (1) molecular structure in petroleum fluid/rock systems with applications in low-salinity-water injection, shale-gas and light-oil reservoirs, improved-oil recovery, and flow assurance and (2) higher-order reservoir simulation. Firoozabadi is the author of *Thermodynamics and Applications in Hydrocarbon Energy Production*, published by McGraw-Hill. He is the recipient of the SPE Anthony F. Lucas Gold Medal and a member of the US National Academy of Engineering. Firoozabadi holds a BS degree from the Abadan Institute of Technology, Abadan, Iran, and MS and PhD degrees from the Illinois Institute of Technology, Chicago, Illinois, followed by post-doctoral work at the University of Michigan. All the degrees are in natural-gas engineering.